

Instability in the system of the distant post-AGB star LS III+52°24 (IRAS 22023+5249)

V.G. Klochkova¹, A.S. Miroshnichenko^{2,3}, V.E. Panchuk¹, N.S. Tavalzhanskaya¹, M.V. Yushkin¹

1 – Special Astrophysical Observatory, RAS, Nizhnij Arkhyz, 369167 Russia,

2 – University of North Carolina at Greensboro, Greensboro, NC, USA,

3 – Pulkovo Astronomical Observatory, Russian Academy of Sciences, St. Petersburg, Russia.

e-mail: Valentina.R11@yandex.ru

May 9, 2022

ABSTRACT

The optical spectra of the B-supergiant LS III +52°24 (IRAS 22023+5249) obtained at the 6-meter telescope with a resolution $R \geq 60000$ in 2010–2021 revealed signs of wind variability and velocity stratification in the extended atmosphere. The $H\alpha$ and $H\beta$ lines have a PCyg type profile; their wind absorption changes position in the range from $V_r = -270$ to -290 km/s. The intensity of the $H\alpha$ emission reaches record values with respect to the local continuum: $I/I_{\text{cont}} \geq 70$. The stationary radial velocity according to the positions of symmetric forbidden emissions and permitted metal emissions was taken as the systemic velocity $V_{\text{sys}} = -149.6 \pm 0.7$ km/s. Based on the positions of absorptions of NII and OII ions, a time variability of the radial velocity in the range from -127.2 to -178.3 km/s was found for the first time for this star. This variability indicates the possible presence of a companion and/or atmospheric pulsations. The change of the oxygen triplet profile OI 7775 Å due to the occurrence of unstable emission was registered. The set of interstellar absorptions of the NaID-lines profile in the range from -10.0 to -167.2 km/s is formed in the Local Arm and subsequent arms of the Galaxy. The distance to the star, $d > 5.3$ kpc, combined with the high systemic velocity indicates that the star is located in the Galaxy beyond the Scutum–Crux arm.

1. Introduction

The results of the IRAS telescope mission have opened to astronomers the sky in infrared light. In particular, some infrared sources were distinguished at high latitudes of the Galaxy. Later they were identified with high luminous stars, mainly at the evolutionary stage after the asymptotic giant branch (further – AGB) (Oudmaijer et al 1992; Oudmaijer 1996; Pottash & Parthasarathy 1998; Hrivnak et al 2009). After the optical identification of the some IRAS sources, a boom in the study of these objects began. The results of the first decade are presented in the well known review (Kwok 1993). Some of the post-AGB supergiants are available to high resolution spectroscopy; the reviews of spectral study performed with the 6-m telescope were published by Klochkova (1999, 2014, 2019).

The post-AGB stage includes far evolved stars with initial masses in the interval $2 \div 8 M_{\odot}$. According to Blöcker (1995), at the previous AGB evolutionary stage, these stars are observed as red supergiants with an effective temperature $T_{\text{eff}} \approx 3000\text{--}4500$ K. The AGB stage for stars of these masses is the final phase with nucleosynthesis in stellar cores. The interest in AGB stars and their closest descendants post-AGB stars is mainly due to the fact that the interiors of these stars in their short-term evolution stage there are physical conditions for the synthesis of heavy metal nuclei and the dredge-up of the fresh products of nuclear reactions into the stellar atmosphere and further into the circumstellar and interstellar medium. As a result of these processes, AGB stars with initial masses below $3\text{--}4 M_{\odot}$ are the main suppliers (over 50%) of all elements heavier than iron synthesized by the s-process, which consists in slow (as compared to β -decay) neutronization of nuclei. The details of the evolution of near-AGB stars and the results of calculations of the synthesis and dredge-up of elements are given by Herwig (2005); Di Criscienzo et al (2016); Liu et al (2018).

In the recent decades, a subgroup of hot supergiants has been selected among post-AGB stars, often with emissions in their spectra, classified as post-AGB stars approaching the planetary nebula phase. A good example is the high-latitude hot star SAO 244567 ($T_{\text{eff}} \geq 35000$ K), for which Parthasarathy et al (1993) concluded, by comparing spectra spaced apart by 50 years, that it is approaching the phase of a young planetary nebula.

The object of this paper is the hot supergiant LS III+52°24 associated with the infrared source IRAS 22023+5249. In early studies, see for example, the objects listed by Hardorp et al (1964) mention this star among the stars emitting in $H\alpha$. The SIMBAD database points the star as spectral type Be. Suárez et al (2006), studying a large sample of stars with IR excesses, classified IRAS 22023+5249 as an object in transition to a planetary nebula.

The main features of the optical spectrum of LS III+52°24 are well known by now. Sarkar et al (2012) used the high resolution spectrum to determine the fundamental parameters of the star and the chemical composition of its atmosphere. Having obtained a large radial velocity from the absorption lines, $V_r = -148.31 \pm 0.60$ km/s, these authors

came to the conclusion that LS III+52°24 is an O-rich post-AGB star. Arkhipova et al (2013) found a fast (from night to night) variability in the UBV bands with a variability amplitude $\Delta V=0.35$ mag. These authors also found a correlation between the star's brightness and the intensity of the H I, He I, [NII], [SII], and other lines; they also noted an increase in the equivalent widths of the [NII] and [SII] nebular emissions over 20 years.

In this paper, we present the results of the optical spectra analysis of LS III +52°24 obtained with the 6-m BTA telescope in 2010–2021. The main goal of our study is to search for the variability in the profiles of spectral features and the behavior of the radial velocity pattern with time. The methods of observation and data analysis are briefly described in Section 2. In Section 3, the results are presented in comparison with those published earlier. The discussion of the results and the conclusions are provided in Section 4.

2. Observations and data processing

Table 1. Results of the measurements of the heliocentric radial velocity V_r in the LS III+52°24 spectra from different types of lines. Columns 4–6, denoted as (abs)/(emis), show V_r from the absorption (top) and emission (bottom) components of the corresponding H α and He I lines.

Date/JD 2450000+	V_r , km/s				
	Absorptions	symmetric emissions	H α (abs)/ (emis)	He I 5876(abs)/ (emis)	He I 6678(abs)/ (emis)
1	2	3	4	5	6
14.07.2001 ¹	−152.4 ±0.3 (8)	−147.3 ±0.17 (15)	−185.36		−182.16
27.09.2010 5467.43	−178.3 ±0.2 (9)	−149.6 ±0.08 (29)	−272.1 −129.7	−228.9 −125.1	−210.5 −121.2
07.12.2019 8825.23	−151.3 ±0.3 (11)	−150.3 ±0.06 (37)	−274.6 −138.2	−229.2 −131.3	−210.0 −125.6
29.08.2020 9091.47	−140.8 ±0.2 (12)	−150.0 ±0.07 (33)	−290.5 : −149.6	−210.7 −121.7	−201.1 −122.5
26.10.2020 9149.27	−127.2 ±0.14 (15)	−148.6 ±0.06 (46)	−271.3 −149.5	−213.3 −122.6	−201.0 −123.2
29.07.2021 9424.52	−141.9 ±0.4 (7)	−150.1 ±0.06 (32)	−273.1 −148.9	−229.4 −123.8	−217.6 −126.5

¹ – V_r values for 2001 year are obtained by averaging the corresponding data by Sarkar et al (2012)

The spectra of LS III+52°24 were obtained with the NES echelle spectrograph (Panchuk et al 2017) positioned at the Nasmyth focus of the 6-meter telescope BTA. The dates of the observations of the star are listed in Table 1. The NES echelle spectrograph is equipped with a large-format CCD with 4608×2048 elements and an element size of 0.0135×0.0135 mm; the readout noise is $1.8e^-$. The registered spectral range is $\Delta\lambda=470\text{--}778$ nm. To reduce light losses without loss of spectral resolution, the NES spectrograph is equipped with an image slicer that splits the image into three slices. Each spectral order in the 2-dimensional image of the spectrum is repeated three times. The spectral resolution is $\lambda/\Delta\lambda \geq 60000$, the S/N ratio along the echelle order in the spectra of LS III+52°24 varies from 40 to 60. One-dimensional data were extracted from two-dimensional echelle spectra using a modified (considering the features of the echelle frames of the spectrograph) ECHELLE context of the MIDAS software package. The details of the procedure are described by Yushkin and Klochkova (2005). The traces of cosmic particles were removed by median averaging of two spectra obtained sequentially one after the other. The wavelength calibration was carried out using the spectra of a Th–Ar lamp with a hollow cathode. All further etapes of processing were performed using the last version of the DECH20t code developed by G. Galazutdinov. The systematic errors in measuring heliocentric velocities V_r estimated from sharp interstellar Na I components and telluric lines do not exceed 0.25 km/s (for one line); the random errors for shallow absorptions are ≈ 0.5 km/s (the average value per one line). For the average V_r values in Table 1, the errors are 0.06–0.3 km/s depending on the number of lines measured. The features in the LS III+52°24 spectrum were identified using the data of Klochkova et al (2002) from the spectral atlas for a hot post-AGB star associated with the IR source IRAS 01005+7910. In addition, we used the results of identifying features in spectra of related objects from the studies of Sarkar et al (2012, 2005). To refine individual data for spectral lines, we also used the data from the VALD database (Ryabchikova et al 2015; Pakhomov et al 2019).

3. Results

3.1. Variability of the optical spectrum of LS III+52°24 and radial velocity patterns

The main features of the optical spectrum of hot post-AGB stars are currently known fairly well. Let us refer to the results of high-resolution spectroscopy published by García-Lario et al (1997), Klochkova et al (2002), Sarkar et al (2012, 2005), Mello et al (2012), and Ikonnikova et al (2020). The optical spectrum of LS III+52°24 is a composition

of the spectrum of a hot supergiant and the emission-rich spectrum of a circumstellar nebula. The spectra contain three types of emissions: the emission component of the complex lines of neutral hydrogen and helium, as well as numerous symmetrical permitted (OI, SiIII, AlIII, CII, FeI, FeII, FeIII) and forbidden low-excitation emissions ([NII], [OI], [SII]). The occurrence of forbidden emissions [NII], [SII] indicates the approach to the planetary nebula phase. The profiles of each of these types of lines are presented in Figs. 1, 2, 3, 4. All forbidden emissions in the [NII] spectrum have the simplest symmetric profile: a narrow Gaussian with a half-width of ≈ 10 km/s. The profiles of forbidden oxygen emissions are more complex.

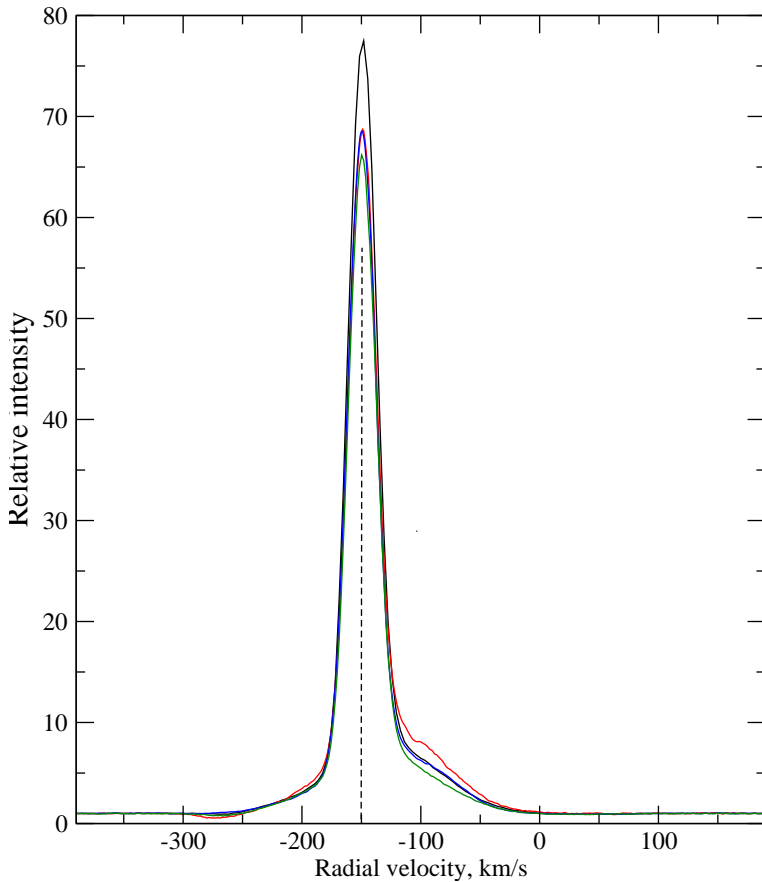


Fig. 1. $H\alpha$ profile in the coordinates of radial velocity versus relative intensity in the LS III+52°24 spectra obtained on September 27, 2010 (red line), December 7, 2019 (green line), August 29, 2020 (blue line), and October 26, 2020 (black line). Here and below, the position of the dashed vertical line coincides with the accepted value of the system velocity $V_{\text{sys}} = -149.6$ km/s.

As follows from Fig. 4, the slopes of the [OI] 6300 Å emission profile are almost vertical and are approximately ± 20 km/s away from the center of the profile. The half-width of the profile of the same emission, but of a telluric origin, is many times lower than ≈ 3 km/s. The [OI] 6300 Å emission profiles presented in Fig. 4 for three observation dates allow us to note the variability of this line, which may reflect the complex structure of the gas envelope of the star.

Table 1 contains the measurement results of the heliocentric radial velocity V_r in the LS III+52°24 spectra from the positions of the samples of various types of lines: absorptions, symmetric forbidden and permitted emissions, emission and absorption components of $H\alpha$ and HeI lines. The numbers in parentheses indicate the number of features used in the averaging. As follows from the data in the table, the velocity from the sample of symmetric emissions formed in the circumstellar envelope does not change for all observation dates. The constancy of this value allows us to take its average as the system velocity of LS III+52°24: $V_{\text{sys}} = -149.6$ km/s.

Multiple observations over a long time period allow us to discover the variability of the positions of pure ion absorptions. As follows from the data in the 2-d column of the table, the average velocity over the sample of absorptions of OII and NII ions varies in the range from -127.2 to -178.3 km/s, which is a manifestation of instability in the deep layers of the stellar atmosphere. This variability may be due to the pulsations in the extended atmosphere of the supergiant or the presence of a companion in the system.

The variability in the intensity of the $H\alpha$ and HeI lines was discovered earlier by Arkhipova et al (2013) from low-resolution spectra. Our observations allow us to refine this result. The $H\alpha$ line profile shown in Fig. 1 in the coordinates of relative intensity versus radial velocity contains a strong emission for all the observation dates. We emphasize that LS III+52°24 holds the record for the emission power in $H\alpha$: as follows from Fig. 1, the $H\alpha$ emission intensity with respect to the local continuum reaches $I/I_{\text{cont}} \geq 70 \div 78$. The position of this emission does not change with time and coincides

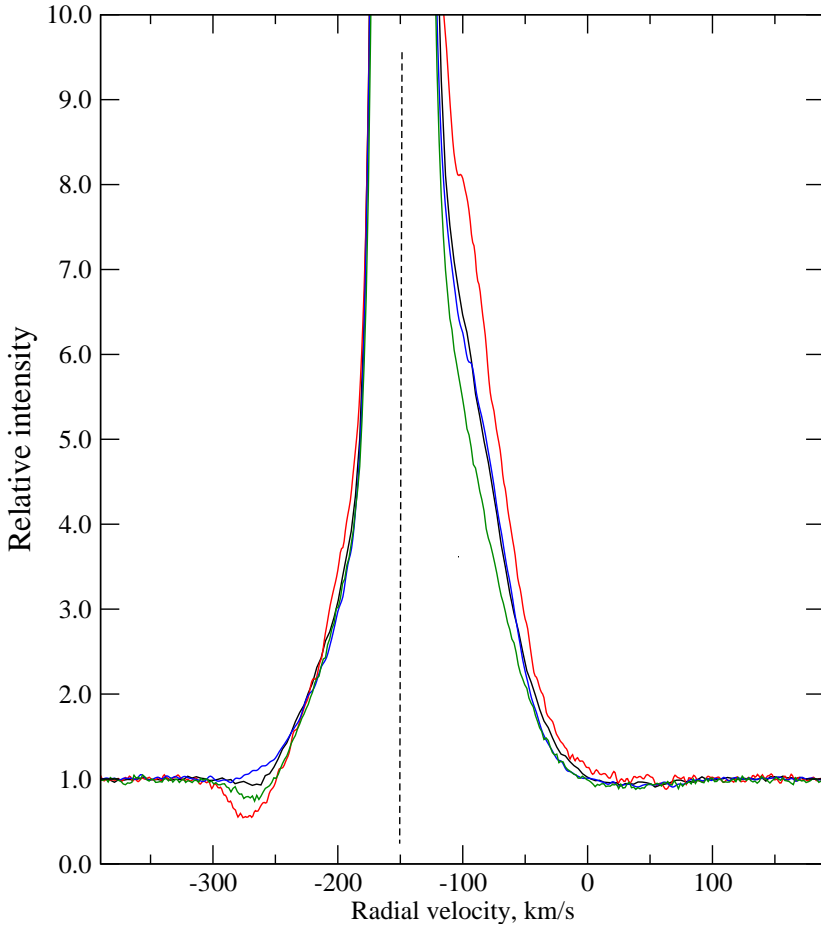


Fig. 2. Same as in Fig. 1 for the lower part of the $H\alpha$ profile

with the system velocity $V_{\text{sys}} = -149.6$ km/s we adopted. The variability of the emission intensity in $H\alpha$ indicates the variability of the stellar wind power and the inhomogeneity of the star’s gas envelope.

Figure 2, which shows the lower fragment of the $H\alpha$ profile, illustrates the shift in the position of the absorption component and the change in the depth of this wind feature, which forms in the upper layers of the outflowing atmosphere at the base of the stellar wind. From the data in the 4-th column of Table 1, the variability range of the wind absorption position is from -270 to -290 km/s. The terminal velocity reaches -300 km/s. The fragment of the $H\alpha$ profile in Fig. 2 clearly shows the presence of a variable additional emission component in the long-wave wing of the $H\alpha$ profile.

The LS III+52°24 spectrum also indicates a significant date-to-date variability of neutral helium lines with profiles of the P Cyg type. To illustrate this phenomenon, Fig. 3 compares the profiles of the He I 6678 Å line in the spectra for three observation dates. Here, we can clearly see the variability of the intensity and position of the emission and absorption components. In this case, the terminal velocity reaches the same values as on the $H\alpha$ profile. Additionally, Fig. 5 shows the profiles of two He I 6678 and 7065 Å lines for two dates of our observations: December 17, 2019 and August 29, 2020. The most interesting and new detail here is the enhancement of wind absorption in He I 6678 Å; at the same time, in August 2020, this kind of wind absorption formed for the first time near the He I 7065 Å line.

In addition, a rare feature was recorded in the spectrum of LS III+52°24: a significant variability in the profile of the infrared oxygen triplet, O I 7775 Å, which is illustrated in Fig. 6, where the triplet profiles for two observation dates are compared. This feature, along with the emission components in the Na I D-lines profile, was mentioned in passing in the paper by Mello et al (2012) dedicated to the spectroscopy of hot post-AGB stars. In addition, Arkhipova et al (2013), give in their Table 8 two values of the total equivalent width of O I 7775 Å emission for the oxygen triplet, which also indicates the variability of the triplet profile.

We also note that the forbidden emissions [S II] 6717 and 6731 Å are systematically shifted to the short-wave region by approximately -20 km/s relative to other forbidden emissions. This feature, due to the stratification of the gas envelope, is preserved in our spectra from date to date. It was previously noted by Sarkar et al (2012) for its 2001 spectrum as well.

3.2. Distance to the star and its Luminosity

The parallax of LS III+52°24 from the Gaia EDR3 catalog, which is measured with high accuracy ($\pi = 0.17313 \pm 0.018$ mas), leads to a large distance to the star: $d = 5.84 \pm 0.6$ kpc. The SIMBAD database shows the parallax from

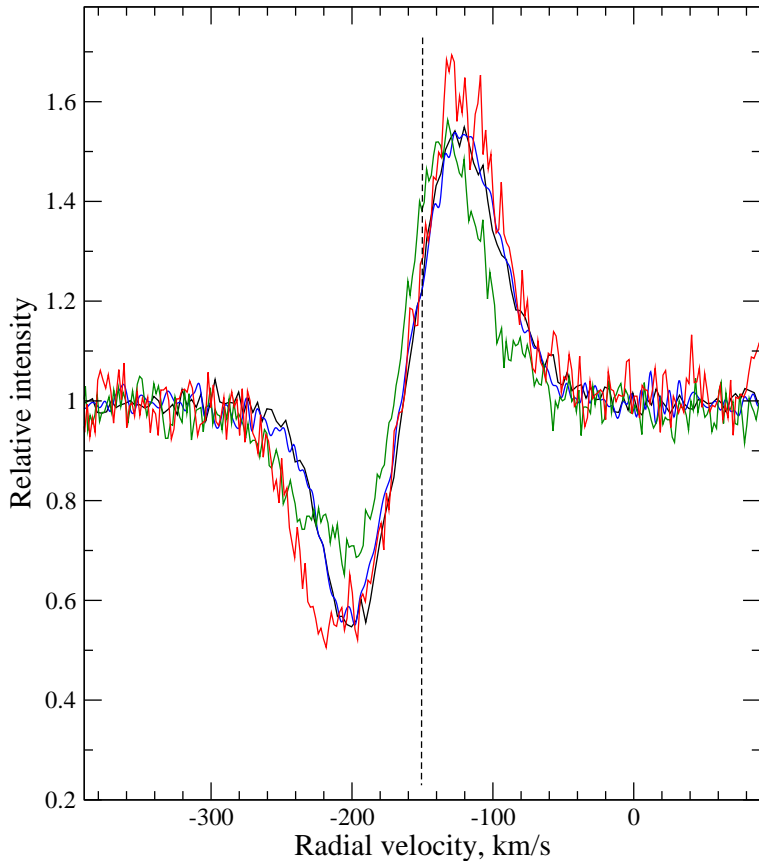


Fig. 3. Same as in Fig. 1 for the He I 6678 Å line.

Gaia DR2, which has too low accuracy, $\pi = 0.0804 \pm 0.0524$ mas. Bailer-Jones et al (2021) refined the parallax $\pi = 0.19$ mas on the basis of modeled Gaia DR3 data, and given the corresponding distance $d = 5.34$ kpc. The significant distance to the star is confirmed by the presence of interstellar components that do not belong to the Local Arm in the structure of the D-lines profile of the Na I doublet. The multicomponent profile of the Na I 5889 Å doublet for two observation dates is shown in Fig. 7. Here, the numbers indicate the components that form in different layers of the circumstellar and interstellar medium. The short vertical lines in this figure indicate the positions of the two interstellar components of the KI 7696 Å line. Absorption components 3–7 in the range of velocities from -10.4 to -56.1 km/s are of interstellar origin. Emission 2 forms in the circumstellar gaseous medium, and its position ≈ -150.2 km/s is consistent with the systemic velocity.

The absorption components of the Na I doublet line profiles (from -10 to -72 km/s) were previously recorded by Klochkova et al (2014) in the spectrum of the central star of the related object IRAS 01005+7910 located above the galactic plane (its latitude $b = +16.6^\circ$). The shortwave absorption “1”, the position of which, $V_r = -170$ km/s, does not change from date to date of observations, probably forms in the circumstellar envelope expanding at a rate of approximately $V_{\text{exp}} = -20$ km/s. This estimate of the envelope expansion velocity does not contradict the values of this parameter from the paper by Sarkar et al (2012), who estimated the expansion rate based on the widths of forbidden lines [NII] and [SII]. The expansion rate from the [OI] 6300 and 6363 Å forbidden line profiles substantially exceeds this parameter, which we also see from our observations. The profile of the [OI] 6300 Å line shown in Fig. 4 is repeatedly wider and, possibly, structured.

It should be noted that the interstellar component $V_r \approx -12$ km/s forming in the Local Arm of the Galaxy was discovered earlier by Klochkova et al (2010) in the spectrum of the post-AGB star V448 Lac (=IRAS 22223+4327). This star has galactic coordinates close to those of LS III+52°24, but a larger parallax, $\pi = 0.2375 \pm 0.0670$ mas; this corresponds to a distance of approximately 4.2 kpc, which is consistent with the distance based on the V448 Lac system velocity from radio observations.

The average velocity for the diffuse interstellar bands (DIBs) identified in the available LS III+52°24 spectra, $V_r(\text{DIBs}) = -16.0 \pm 0.2$ km/s, is consistent with the velocity for the Na I and KI interstellar components. To estimate the interstellar extinction, we used the equivalent widths W_λ of the DIBs available in our spectra and the ratios between the color excess, $E(B-V)$, and W_λ according to the calibrations from (Kos and Zwitter 2013). Table 2 shows the W_λ values averaged over our spectra, and the corresponding color excesses are given in the last column. For two lines absent in the publication by Kos and Zwitter (2013), the $E(B-V)$ values in italics were obtained using the calibration dependences from Luna et al (2008). The average over eight DIBs $E(B-V) = 0.33$ mag. This estimate of reddening agrees well with the interstellar reddening from (Green et al 2019) near the Galactic plane in the direction of the Scutum–Crux arm.

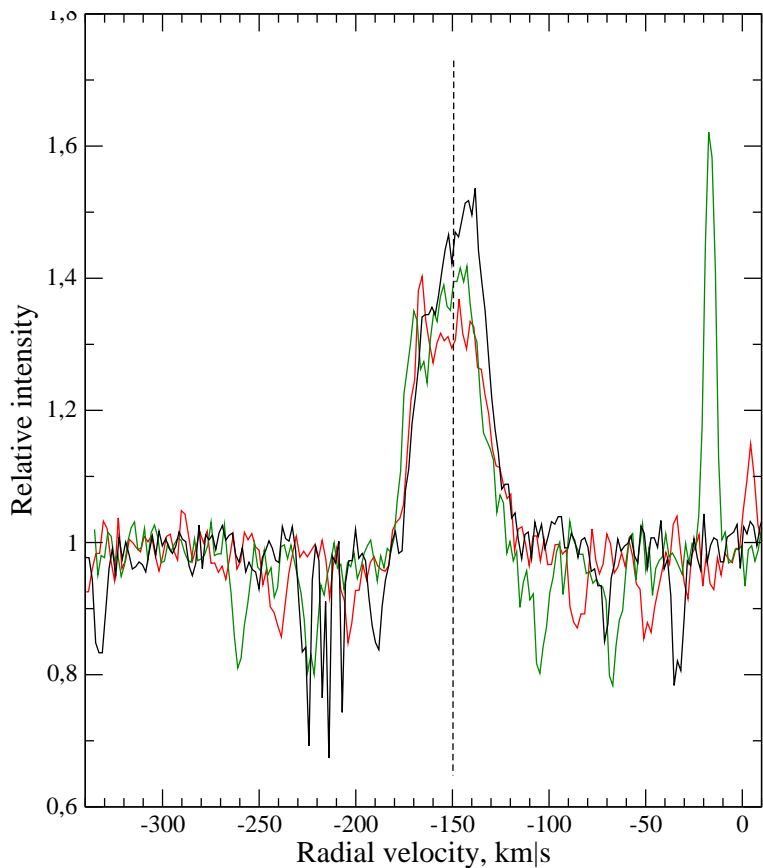


Fig. 4. Profile of the [OI] 6300 Å line in the LS III+52°24 spectra taken on September 27, 2010 (red line), December 7, 2019 (green line), and July 29, 2021 (black line). The narrow emissions in this fragment are the [OI] 6300 Å telluric line

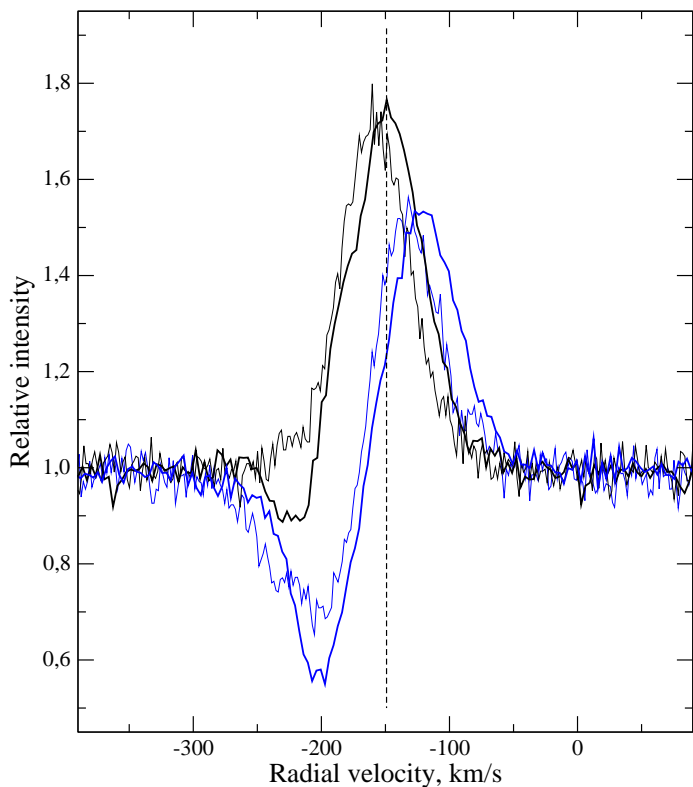


Fig. 5. Variability of the He I 6678 (blue lines) and He I 7065 Å (black lines) line profiles in the LS III+52°24 spectra taken on December 7, 2019 (thin lines) and August 29, 2020 (thick lines).

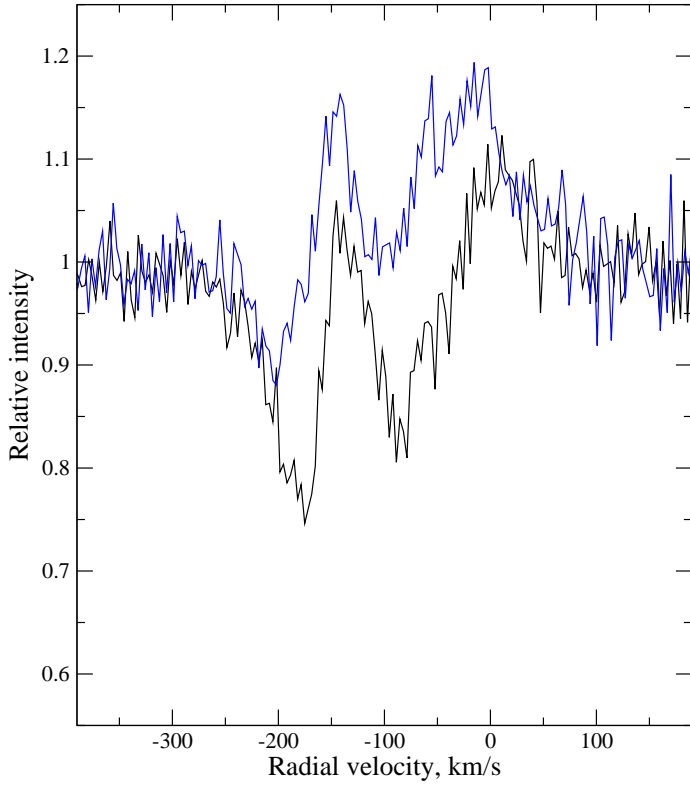


Fig. 6. Profile of the OI 7775 Å triplet in the LSIII+52°24 spectra taken on August 29, 2020 (blue line) and October 26, 2020 (black line).

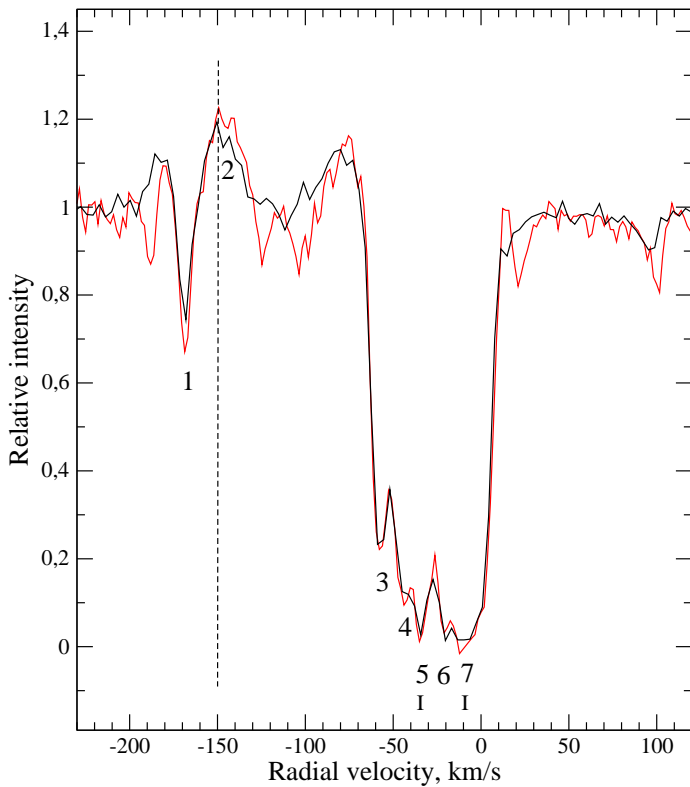


Fig. 7. Multicomponent profile of the NaI 5889 Å line in the LSIII+52°24 spectra taken on August 29, 2020 (black line) and October 26, 2020 (red line). Two short verticals correspond to the velocities of the interstellar components of the KI 7696 Å line.

The estimate of reddening $E(B-V)$ we obtained for LSIII+52°24 is two times lower than the value $E(B-V)=0.66$ mag from (Arhipova et al 2013). Such a significant difference is due to the difference in methods for assessing the reddening. In our case, the estimate was made on the basis of the equivalent widths of interstellar bands measured in the spectrum,

and in Arkhipova et al (2013) the reddening was determined by comparing the observed colors (U-B) and (B-V) with the normal colors of standard supergiants of the corresponding spectral class. Thus, an estimate was obtained for the total color excess due to the total absorption in the interstellar medium and the circumstellar envelope of the star. Such a significant difference in color excess due to interstellar and total extinction is a typical property for post-AGB stars (see the sample of related post-AGB stars in the paper by Gauba et al (2003) as an example).

Table 2. Equivalent widths of DIBs in the LS III+52°24 spectra. The third column indicates the corresponding color excesses obtained using the calibrations by Kos and Zwitter (2013); the values according to the calibrations by Luna et al (2008) are italicized.

λ , Å	W_λ , mÅ	E(B-V) mag
5780.48	334	0.56
5797.06	58	0.29
6195.98	22	0.33
6283.84	496	<i>0.55</i>
6379.32	17	0.15
6613.62	62	0.24
6660.71	19	0.40
7224.03	132	<i>0.53</i>

Using the standard ratio of the total absorption to the color excess, $R=3.2$, and the color excess from the data of Arkhipova et al (2013), we obtain the total absorption for LS III+52°24 $A_v=2.11$ mag. Having a reliable distance to the star ($d=5.8$ kpc) and total extinction, as well as using the effective temperature $T_{\text{eff}}=24000$ K published by (Sarkar et al 2012) and the bolometric correction $BC_V = -2.5$, corresponding to this temperature, we can estimate the bolometric magnitude $M_{\text{bol}}=-5.9$ mag and luminosity of the star $\log L/L_\odot=4.27$. The parallax-based luminosity from Bailer-Jones et al (2021) is slightly lower: $\log L/L_\odot=4.18$. Taking into account the 1000 K uncertainty of the effective temperature (Sarkar et al 2012), we arrive at the average value of the luminosity $\log L/L_\odot = 4.2 \pm 0.3$.

The data from (Parthasarathy et al 2020) indicate that the luminosity of LS III+52°24 obtained by us is typical of a post-AGB star. It should be taken into account that Parthasarathy et al (2020) estimated the parameters for the post-AGB sample using the star parallaxes from Gaia DR2 and gave only the lower bound for the luminosity estimate for LS III+52°24. It should be noted that the real luminosity of LS III+52°24 may be slightly lower if we consider that the apparent brightness of the star is enhanced due to the presence of powerful emissions in its spectrum.

The luminosity we obtained $\log L/L_\odot = 4.2 \pm 0.3$ serves as an additional indication that the star does not belong to the supergiants with the B[e] phenomenon, the luminosity of which is much higher. According to Miroshnichenko (2007), the average luminosity for a sample of this type of supergiants in the Galaxy is higher: $\log L/L_\odot = 5.1 \pm 0.2$.

4. Discussion of the results and conclusions

The observed variability of the absorption–emission profiles of HI and HeI lines in the spectrum of LS III+52°24 indicates the inhomogeneity and the presence of structure in its circumstellar gaseous envelope. This inhomogeneity and the absence of spherical symmetry are also recorded in the near-IR images of IRAS 22023+5249 obtained by Gledhill and Forde (2015) with the NIFS instrument of the 8.2-meter Gemini North telescope. The spectrum of the extended gaseous envelope contains a rich spectrum of molecular hydrogen; the HI and HeI emissions have profiles of the P Cyg type. The image in the Br γ band is especially informative, where, as Gledhill and Forde (2015) emphasize, there is a strong central emission peak, an additional elliptical envelope, as well as bright spots and curved features. Such a structured circumstellar medium can also explain the occurrence and variability of additional emission in the longwave wing of the H α profile in our Fig. 2.

An unexpected property of the supergiant LS III+52°24 is its high system velocity, $V_{\text{sys}}=-149.6 \pm 0.7$ km/s. This feature is the decisive argument for the fact that the star belongs to the old population of the Galaxy. This high velocity is consistent with the large remoteness of the star, $d>5.3$ kpc, obtained from its rather reliable parallax according to the Gaia DR3 data. Invoking the radial velocity mapping in the Galaxy (Vallee 2008), it can be seen that the system velocity for LS III+52°24 (galactic coordinates $l \approx 100^\circ$, $b \approx -2^\circ$) and its large distance are in good agreement with the fact that the star belongs to the space beyond the Scutum–Crux arm.

There are other objects in the family of hot post-AGB stars with similarly high velocities. For example, a significant $V_r=-124.2 \pm 0.4$ km/s was determined by Ikonnikova et al (2020) for the post-AGB star LS 5112 (IRAS 18379–1707). The combination of fundamental parameters and spectral features of LS 5112 obtained by Ikonnikova et al (2020) allows us to consider this star as the closest analog of LS III+52°24. We regard the revealed excess of helium and CNO elements as an important result of these authors, which directly indicates the post-AGB evolution stage and the effectiveness of the third dredge-up that took place. Unfortunately, it is not possible to compare the behavior of the spectral features of LS 5112 and LS III+52°24 over time, since the LS 5112 spectrum was studied by Ikonnikova et al (2020) based on a single observation. A related object is the hot post-AGB star V886 Her (=IRAS 18062+2410), for which (Arkhipova et al 2001a) found a photometric variability of the same amplitude, identified a set of forbidden emissions, as well as HeI wind

components. The closest relative of this star is the hot B-supergiant LS II+34°26 (= V1853 Cyg), in the spectrum of which Arkhipova et al (2001b) identified many envelope emissions and recorded the systemic velocity of approximately -49 ± 5 km/s.

As noted in the Introduction, the high-resolution optical spectrum of LS III+52°24 was studied earlier in detail by Sarkar et al (2012). These authors were the first to determine its fundamental parameters, the chemical composition of its atmosphere; they also found a high radial velocity from absorption lines, $V_r = -148.31 \pm 0.60$ km/s, and documented the status of the star as an O-rich post-AGB star. But that study was also based on a single observation. Apparently, the time behavior of the optical spectrum in the family of hot post-AGB stars has been studied on the basis of high spectral resolution observations only for IRAS 01005+7910 (Klochkova et al 2002, 2014) so far, which located slightly closer in the Galaxy according to its reliable parallax $\pi = 0.2414 \pm 0.0176$ mas from Gaia DR3.

We should note that the abovementioned features of the optical spectrum of LS III+52°24 (powerful emissions of HI and HeI lines with variability in profiles, the presence of forbidden emissions of light metal ions), as well as its position near the plane of the Galaxy (galactic latitude $b = -1.96^\circ$) allow us to suspect that this star belongs to the family of supergiants with the B[e] phenomenon, the principal features of the spectra of which were provided by Lamers et al (1998). A good example of a supergiant with the B[e] phenomenon is MWC 17, a hot star several kiloparsecs away in the system of the source IRAS 01441+6026 near the Galactic plane. As shown by Klochkova and Chentsov (2018), the optical spectrum of MWC 17 contains powerful HI emissions and is rich with intense forbidden and permitted metal emissions, while stellar absorptions are absent completely, with the exception of interstellar absorptions of the NaI D-lines and DIBs. However, the total set of available data for LS III+52°24 (low absolute luminosity, chemical composition features according to the data by Sarkar et al (2012), and high radial velocity) corresponds to the status of a hot post-AGB star. Thus, the spectrum of the supergiant LS III+52°24 is an example of spectral mimicry of supergiants. This phenomenon was previously considered in more detail by Klochkova and Chentsov (2018).

The powerful $H\alpha$ emission in the spectrum of LS III+52°24 is 65–77 times higher than the level of the local continuum. Such a powerful emission in $H\alpha$ is a unique phenomenon for low-mass supergiants. As follows from the papers by Arkhipova et al (2001b), Klochkova et al (2002, 2014) and Ikonnikova et al (2020), the $H\alpha$ emission intensity in the spectra of the closest analogs, hot central post-AGB stars in the IR-source systems IRAS 01005+7910, IRAS 18062+241, and IRAS 18379–1707 is an order of magnitude lower. Even in the spectra of supergiants with the B[e] phenomenon, the $H\alpha$ emission is also significantly lower (see the examples of profiles in the spectra of supergiants with the B[e] phenomenon in papers by Klochkova and Chentsov (2016); Miroshnichenko et al (2009, 2021)). Such a strong $H\alpha$ emission can rather be seen in the spectra of stars of extremely high luminosity, for example, in the LBV spectra. However, even the spectrum of star No12 in the Cyg OB2 association, which is a well-known candidate for LBV, the $H\alpha$ intensity many times lower than that observed in the spectrum of LS III+52°24, the luminosity of which is much lower. Apparently, this phenomenon is due to the significant contribution of the circumstellar gaseous medium and is related to the problem of spectral mimicry of supergiants (Klochkova and Chentsov 2018). The absence of an excess flux in the near-IR range and the high systemic velocity, $V_{\text{sys}} \approx -150$ km/s determined by us confirm the conclusion by Sarkar et al (2012) that LS III+52°24 belongs to the type of low-mass supergiants at the post-AGB stage approaching the planetary nebulae.

The main new results obtained from multiple observations of the B-supergiant LS III+52°24 in a wide wavelength range in 2010–2021 are as follows:

- reliable record of the LS III+52°24 systemic velocity from stationary emissions in its spectrum: $V_{\text{sys}} = -149.6 \pm 0.7$ km/s;
- conclusion about the significant distance to the star, $d \approx 5.3$ kpc;
- detection of the velocity variability and stratification in the extended atmosphere and the unhomogeneous envelope. The position of wind absorption changes in the interval from -270 to -290 km/s. The wind speed reaches 150 km/s;
- detection of the time variability of the radial velocity based on the positions of photospheric absorptions of NII and OII ions in the range from -127.2 to -178.3 km/s, which indicates the presence of a component or pulsations in the atmosphere;
- discovery of the variability of the profile of the oxygen IR triplet OI 7775 Å due to the appearance of unstable emission.

It is obvious that finding the cause and determining the parameters of the detected variability in the radial velocity and line profiles will require further spectral monitoring of LS III+52°24 with a high spectral resolution.

Acknowledges

V.G.K., who performed the analysis of the spectra and kinematic data for the LS III+52°24 system, thanks the Russian Science Foundation for support (grant no. 22-22-00043). The observations with telescopes of the Special Astrophysical Observatory, Russian Academy of Sciences, were supported by the Ministry of Science and Higher Education of the Russian Federation (agreement no. 05.619.21.0016, project id. RFMEFI61919X0016). The study used the SIMBAD, VALD, SAO/NASA ADS, and Gaia DR3 astronomical databases.

References

- V.P. Arkhipova, V.G. Klochkova, G.V. Sokol, *Astronomy Letters* **27**, 99 (2001a).
- V.P. Arkhipova, N. P. Ikonnikova, R. I, Noskova, G. V. Komissarova, V. G. Klochkova, V. F. Esipov, *Astronomy Letters* **27**, 841 (2001b).
- V.P. Arkhipova, M.A. Burlak, V.A. Esipov, N.P. Ikonnikova, G.V. Komissarova, *Astronomy Letters* **39**, 619 (2013).
- C.A.L. Bailer-Jones, J. Rybizki, M. Fouesneau, M. Demleitner, R. Andrae, *AJ* **161** (3) 147 (2021).
- T. Blöcker, *A&A* **297**, 727 (1995).
- M. Di Criscienzo, P. Ventura, D.A. García-Hernández, F. Dell’Agli, M. Castellani, P.M. Marrese, S. Marinoni, G. Giuffrida, O. Zamora, *MNRAS* **462**, 395 (2016).
- P. García-Lario, M. Parthasarathy, D. de Martino, L. Sanz Fernandez de Cordoba, R. Monier, A. Manchado, S.R. Pottasch, *A&A* **326**, 11037 (1997).
- G. Gauba, M. Parthasarathy, B. Kumar, R.K.S. Yadav, R. Sagar, *A&A* **404**, 305 (2003).
- T.M. Gledhill, K.P. Forde, *MNRAS* **447**, 1080 (2015).
- G.M. Green, E. Schlafly, C. Zucker, J.S. Speagle, D. Finkbeiner, *ApJ* **887**, (1) id.93 (2019).
- J. Hardorp, I. Theile, H.H. Vogt, *Hamburger Sternw., Warner & Swasey Obs.*, **3**, 0, (1964).
- F. Herwig, *ARA&A* **43**, 435 (2005).
- B.J. Hrivnak, K. Volk, S. Kwok, *ApJ* **694**, 1147 (2009).
- R.D. Oudmaijer, W.E.C.J. van der Veen, L. B. F. M. Waters, et al *Astron. and Astrophys. Suppl.* **96**, 625 (1992).
- R.D. Oudmaijer, *A&A* **306**, 823 (1996).
- N.P. Ikonnikova, M. Parthasarathy, A.V. Dodin, S. Hubrig, G. Sarkar, *MNRAS* **491**, 4828 (2020)
- V.G. Klochkova, *Bull. Spec. Astrophys. Obs.* **44**, 5 (1999).
- V.G. Klochkova, *Astrophys. Bull.*, **69**, 279 (2014).
- V.G. Klochkova, *Astrophys. Bull.*, **74**, 475 (2019).
- V.G. Klochkova & E.L. Chentsov, *Astrophys. Bull.*, **71**, 33 (2016).
- V.G. Klochkova, E.L. Chentsov, *Astronomy Reports* **62**, (1) 19 (2018).
- V.G. Klochkova, M.V. Yushkin, A.S. Miroshnichenko, V.E. Panchuk, K.S. Bjorkman, *A&A* **392**, 143 (2002).
- V.G. Klochkova, V. E. Panchuk, N. S. Tavalzhanskaya, *Astronomy Reports* **54**, 234 (2010).
- V.G. Klochkova, E.L. Chentsov, V.E. Panchuk, E.G. Sendzikas, M.V. Yushkin, *Astrophys. Bull.*, **69**, 439 (2014).
- J. Kos & T. Zwitter, *ApJ* **774**, 72 (2013).
- S. Kwok, *ARA&A* **31**, 63 (1993).
- H.J.G.L.M. Lamers, F.J. Zickgraf, D. de Winter, L. Houziaux, J. Zorec, *A&A* **340**, 117 (1998).
- N. Liu, R. Gallino, S. Bisterzo, A.M. Davis, R. Trappitsch, L.R. Nittler, *ApJ* **865**, 112 (2018).
- R. Luna, R.N.L.J. Cox, M.A. Satorre, D.A. García Hernández, O. Suárez, P. Garcà Lario, *A&A* **480**, (1) 133 (2008).
- M. Mello, S. Dafton, C.B. Pereira, I. Hubeny, *A&A* **543** A11 (2012).
- A.S. Miroshnichenko, *ApJ* **667**, 497 (2007).
- A.S. Miroshnichenko, E.L. Chentsov, V.G. Klochkova, S.V. Zharikov, K.N. Grankin, A.V. Kusakina, T.L. Gandet, G. Klingenberg, S. Kildahl, R.J. Rudy, D.K. Lynch, C.C. Venturini, S. Mazuk, R.C. Puetter, R.B. Perry, A.C. Carciofi, K.S. Bjorkman, R.O. Gray, S. Bernabei, V.F. Polcaro, R.F. Viotti, L. Norci, *ApJ* **700**, 209 (2009).
- A.S. Miroshnichenko, V.G. Klochkova, E.L. Chentsov, V.E. Panchuk, M.V. Yushkin and N. Manset, *MNRAS* **507**, 879 (2021).
- Yu.V. Pakhomov, T.A. Ryabchikova, N.E. Piskunov, *Astronomy Reports* **63**, 1010 (2019).
- V.E. Panchuk, V.G. Klochkova, M.V. Yushkin, *Astronomy Reports* **61**, 820 (2017).
- M. Parthasarathy, P. Garcia-Lario, S.R. Pottasch, A. Manchado, J. Clavel, D. de Martino, G.C.M. van de Steene, K.C. Sahu, *A&A* **267**, L19 (1993).
- M. Parthasarathy, T. Matsuno, W. Aoki, *PASJ* **72** (6) 99 (2020).
- S.R. Pottash, M. Parthasarathy, *A&A* **192**, 182 (1998).
- T. Ryabchikova, N. Piskunov, R.L. Kurucz, H.C. Stempels, U. Heiter, Yu. Pakhomov, P.S. Barklem, *Physica Scripta*, **90**, (5) article id. 054005 (2015).
- G. Sarkar, M. Parthasarathy, B.E. Reddy, *A&A* **431**, 1007 (2005).
- G. Sarkar, D. A. García-Hernández, M. Parthasarathy, A. Manchado, P. Garcia-Lario, Y. Takeda, *MNRAS* **421**, 679 (2012).
- O. Suárez, P. García-Lario, A. Manchado, M. Manteiga, A. Ulla, S.R. Pottasch, *A&A* **458**, 173 (2006).
- J.P. Vallee, *AJ* **135**, 1310 (2008).
- M.V. Yushkin and V.G. Klochkova, *Special Astrophysical Observatory, Preprint No. 206*, (2005).